

**Vertical graphene nanoflakes for the immobilization, electrocatalytic oxidation and quantitative detection of DNA**

*Naigui Shang,<sup>1,3,\*</sup> Ajay Kumar,<sup>1</sup> Nijuan Sun,<sup>2</sup> Surbhi Sharma,<sup>1</sup> Pagona Papakonstantinou,<sup>1,\*</sup>  
Meixian Li,<sup>2</sup> Ross A. Blackley,<sup>4</sup> Wuzong Zhou,<sup>4</sup> Lisa S. Karlsson,<sup>5</sup> S. Ravi P. Silva<sup>3</sup>*

<sup>1</sup>Nanotechnology and Integrated Bio-Engineering Centre, University of Ulster, Newtownabbey,  
BT37 0QB, UK

<sup>2</sup>College of Chemistry and Molecular Engineering, Peking University, Beijing 100871, China

<sup>3</sup>Advanced Technology Institute, University of Surrey, Guildford, GU2 7XH, UK

<sup>4</sup>School of Chemistry, University of St Andrews, St Andrews, KY16 9ST, UK

<sup>5</sup>Department of Materials, University of Oxford, Oxford, OX1 3PH, UK

\*Address correspondence to [ngshang@hotmail.com](mailto:ngshang@hotmail.com) and [p.papakonstantinou@ulster.ac.uk](mailto:p.papakonstantinou@ulster.ac.uk)

**Abstract**

Vertical graphene nanoflake integrated films having a high density of edge planes have been used as an electrochemical platform to systematically investigate the immobilization, electrochemical oxidation kinetics and direct quantitative determination of natural DNA. Consistently, both transmission electron microscopy and atomic force microscopy observations demonstrate the presence of a self-assembled monolayer of native DNA, immobilized on the graphene nanoflakes. Graphene shows excellent electrocatalytic activity for the electrooxidation of double stranded DNA, better than carbon nanotubes and glassy carbon, due to the abundance of electrocatalytic graphene edges present not only at the top but also along the sides of each graphene nanoflake.

**Keywords:** graphene nanoflake, DNA, electrocatalytic oxidation, AFM, TEM

## 1. Introduction

Given the exceptional promise of graphene as a transduction element in analytic and biosensing devices efforts have been directed on interfacing graphene with various types of biological systems.<sup>1-4</sup> Interest in the electrochemistry of double stranded (ds) DNA has been spurred by their relevance to oxidative damage, detection of mutations and design of therapeutic drugs.<sup>5-8</sup> To date, various electroanalytical approaches have been reported including direct oxidation of DNA bases and indirect oxidation through the use of electroactive mediators, which involves intercalation of redox probe molecules to report perturbations in the  $\pi$ -stacked base pairs within dsDNA. Of these, direct oxidation of DNA is the simplest one. Except for the latest reported chemically reduced graphene oxide,<sup>9,10</sup> essentially for all other popular electrodes such as gold,<sup>11</sup> glassy carbon (GC),<sup>12</sup> CNT<sup>13,14</sup>, polymer modified graphite/GC<sup>15</sup> and pyrolytic graphite electrode<sup>16</sup> only the adenine (A) and guanine (G) residues of the dsDNA can electrochemically be oxidized with a poor signal and a low sensitivity. **The reason for the reduced graphene oxide being able to detect the four bases of dsDNA could be either the formation of a mixture of single-layer and few-layer sheets which contains highly actively single-layer atomic edge sites,<sup>17, 18</sup> or different levels of oxygen contents in formed single/few-layer sheets which significantly lower the barrier of DNA oxidation.**<sup>19</sup> Currently, due to the different electrochemical activity and assays employed, the mechanism of the electrooxidation of dsDNA based on different electrodes is not clear and the interaction of DNA with electrodes has a non consistent behavior. For example, Bollo et al.,<sup>12</sup> Pedano et al.<sup>20</sup> and Nowicka et al.<sup>21</sup> found that dsDNA exhibits weak responses at polished GC electrodes, while two other research groups reported no electrochemical response of dsDNA at bare GC electrodes.<sup>13, 22, 23</sup> Obviously, this points to the fact that the oxidation dynamics of dsDNA on such electrodes could relate with unknown factors such as the surface roughness, surface functional species, surface area, surface charge, preferential facets, grain size,

electroactive media, time of exposure to air etch, many of which are difficult to be controlled by simple mechanical polishing or electrochemical activation procedures. As for electrodes modified with substances capable of catalyzing the reaction of nucleic bases, their reproducibility is highly variable, due to the difficulty in controlling the quantity, thickness and active surface area of catalytic media by a simple method such as the drop casting or dip coating etc. Therefore, it is necessary to develop novel electrode materials for DNA lab-on-a-chip systems with well-defined morphology.

Recently, high-quality graphene nanoflakes integrated films (GNFs),<sup>24</sup> which are terminated with vertically aligned ultrathin graphene edges have been reported. They possess the combined advantages of large surface area, highly electrochemical activity, stable mechanical strength, and have demonstrated excellent electron transfer properties, highly electrocatalytic activity and good selectivity for a number of biomolecules. In this paper, we use GNFs as an electrochemical platform to systematically investigate the immobilization, electrochemical oxidation kinetics and direct quantitative determination of natural DNA, by means of atomic force microscopy (AFM), high resolution transmission electron microscopy (HRTEM), cyclic voltammetry (CV) and differential pulse voltammetry (DPV).

## **2. Experimental**

Fish sperm DNA from Acros and calf thymus DNA from Beijing Baitai Biochemical Corporation were used without further purification. Both DNA solutions dissolved in 0.2 M NaCl and have a UV absorbance ratio of about 1.8 at 260 and 280 nm, confirming both DNA are of high purity and free of protein.<sup>13</sup>

Uniform GNFs were deposited on highly doped Si wafers by using microwave plasma assisted chemical vapor deposition.<sup>24</sup> The GNFs with and without the immobilized DNA were characterized by AFM and HRTEM. Electrochemical measurements were carried out by using a self-made 10mL cylinder cell. GNFs and a Pt wire were used as the working electrode and auxiliary electrode, respectively. The reference electrode is either a commercial 3M NaCl Ag/AgCl electrode or a Ag/AgCl wire with a supporting solution mixture of 0.2 M NaCl and KCl, whose potentials in our results are calibrated into the commercial standard one. Prior to measurements, all solutions were degassed by flowing pure N<sub>2</sub> for 10 min and were kept under a N<sub>2</sub> ambient throughout the measurement.

### 3. Results and discussion

Figure 1a shows a typical AFM image of GNFs. It was found the GNFs present a robust net-like structure with a large quantity of vertical graphene nanoflakes interlaced together. Each nanoflake resembles a narrow belt with a thick graphitic base that progressively decreases along its altitude terminating finally on a 2–3-nm-thick sharp knife-edge.<sup>24</sup> The knife-edge single crystalline structure is evidenced by the HRTEM images and selected area electron diffraction (SAED) patterns shown in Figure 1b. Thus, the characteristic topological structure of GNFs provides an ideal site for anchoring long ribbon-like DNA. Figure 1c shows an AFM image of dsDNA immobilized GNF electrodes. The GNFs were simply immersed in a typical dsDNA solution (10 mM, pH7.4 phosphate buffer solution with 0.5 mg mL<sup>-1</sup> dsDNA), without using an electrostatic potential, for 5 min in order to immobilize dsDNA and then rinsed by double de-ionized water for several times. This procedure ensures the removal of weakly bound DNA from the graphene surface. It can be seen that the DNA has completely covered the surface of GNFs, not only the sharp edge planes but also the profiles of the nested graphene nanoflakes. This is

further supported by HRTEM observations, which reveal that the graphene sheets are surrounded with a self assembled, monolayer of around 1.5–2.5 nm thick dsDNA. The average interplane distance in different pristine GNFs is about 0.345 nm, while the DNA covering individual graphene nanoflake displays a wide range of lattice spacings ranging from 0.334 to 0.355 nm. This larger variation of lattice constants and the branching of GNFs lively visualize the situation of rigid dsDNA being tightly adsorbed to graphene, which was found to be quite stable under the electron beam irradiation. These findings clearly demonstrate the presence of strong interactions between the graphene layer and the DNA helix possibly with a non-covalent  $\pi$ - $\pi$  stacking similar to the case of DNA wrapped CNTs and highly oriented pyrolytic graphite.<sup>25, 26</sup>

GNF electrodes present an irreversible electrochemical response to dsDNA without a reduction peak at negative scan potentials. Figure 2a shows typical CV profiles of GC and GNF electrodes in the typical dsDNA solution in open circuit, for an accumulation time of 5 min. It is clear that no peaks were observed at the GC electrode, whereas the GNF electrode presents excellent electrocatalytic activity for the electro-oxidation of DNA with two small peaks located at about  $0.70\pm 0.02$  V and  $0.97\pm 0.02$  V, corresponding to the electrochemical oxidation of guanine and adenine residues of dsDNA, respectively.<sup>13, 27</sup> These were further confirmed by a control experiment using other chemical routes such as denatured DNA, guanine, adenine and their mixture solution as shown in Figure 2b.<sup>13</sup> **The denatured DNA was produced by heating natural DNA in a boiling water bath for 10 min. followed by rapid cooling in an ice bath and confirmed by using UV absorption spectrometer with a UV absorbance ratio at 260 and 280 nm of more than that for the original natural DNA. A stronger signal from denatured DNA was found and believed because its open base and structural flexibility enable denatured DNA easily contact the electrode surface.<sup>28</sup> Meanwhile, the ratio of the oxidation A and G peaks for dsDNA is quite**

different from that for denatured DNA, evidencing the denaturation of dsDNA.<sup>29</sup> Compared to single/multi wall CNT modified GC electrodes (pH 7.0–7.2),<sup>13, 14</sup> the oxidation potential of two peaks at GNF electrodes negatively shifts by approximately 50–70 mV, revealing a better electro-catalytic property of graphenes than that of CNTs. In addition, we have measured more than 10 GNF samples and found that they exhibited a high reproducibility for the native DNA electrochemical oxidation. Another advantage of GNFs as an electrode is that they can be repeatedly used after re-constructing a fresh electrode surface by undergoing successive CV scans for a second time in the blank or DNA solution. No fouling effects were observed in the experiment for long durations.<sup>24</sup>

The immobilization of DNA at electrodes is an important subject. Here, the DNA immobilization is to simply immerse GNFs into the DNA solution for the times without using a potential. Figure 2c shows the CV data of G and A peaks at GNF electrodes as a function of the accumulation time. It can be observed that the peak current of two peaks essentially increases with accumulation time and then levels off after a period, for the given concentration of DNA. Boltzmann line fits show the time windows of adsorption balance of the DNA accumulation are in the range of 2.5–5.0 and 2.5–7.5 min. for G and A peaks, respectively. This suggests that the accumulation time of 5 min is optimal, with the DNA adsorption being at a state of dynamic balance throughout the entire electrode surface, rendering the electrode to its most efficient state. To study the kinetics of the electrochemical oxidation, CV profiles of a GNF electrode in a 0.5 mg mL<sup>-1</sup> dsDNA solution were collected at an accumulation time of 5 min. using different scan rates from 200 to 1000 mV s<sup>-1</sup>. Figure 2d shows the CV peak currents versus the scan rate. Both A and G peaks present a perfect linear relation with the scan rate in the range of 200–1000 mV s<sup>-1</sup>, revealing the electrochemical oxidation occurs via an absorption controlled process between GNF and DNA.

This process is similar to that of DNA on the Au electrode, where the electrooxidation reaction is absorption controlled process, being strongly dependant on the scan rate.<sup>11</sup>

DPV is a widely acceptable method to study the detection limit of electrodes due to its high sensitivity. Typical DPV curves taken from GNF electrodes in blank and 80  $\mu\text{g mL}^{-1}$  dsDNA solutions at the accumulation time of 5 min. are shown in Figure 2e. Similar to CV curves, DPV profiles demonstrate only two small peaks: a G peak and an A peak, due to the oxidation of guanine and adenine bases of dsDNA, respectively. Figure 2f shows DPV peak current intensities ( $I_{\text{DPV}}$ ) of peak G as a function of the dsDNA solution concentration ( $C_{\text{DNA}}$ ). It can be fitted by a linear regression equation ( $I_{\text{DPV}} = 0.042 * C_{\text{DNA}} + 0.169$ ) with a correlation coefficient of 0.996. The minimum detectable concentration of dsDNA is approximately 1  $\mu\text{g mL}^{-1}$ . From the fit curve, a lower theoretical detection concentration could be achieved being comparable with that of GC electrodes, where an additional electrostatic preconcentration process for improving DNA immobilization and a more elaborate measurement technique were employed.<sup>21</sup> However, its detection capacity is poorer than that of polypyrrole nanofiber modified graphite electrode via a potentiostatic procedure,<sup>15</sup> possibly because polypyrrole nanofibers have high biological activity, high ion-exchange capacity and strong adsorptive capabilities leading to an improved interaction with DNA compared to graphene.<sup>30</sup>

The excellent electrocatalytic activity and characteristic oxidation dynamics of GNFs for the oxidation of nucleic bases compared to GC and CNT electrodes are accredited to their following unique attributes: (i) The nest-like surface structure of GNFs with large surface area facilitates the anchoring of a high density of DNA with ample contact points between graphene and DNA bases and hence shortens the electron transfer distances; (ii) GNFs possess a high density of



exposed graphene edge planes along both sides of the nanoflakes. Due to their electrocatalytic nature,<sup>31</sup> these edges with plentiful defects are able to access the electroactive centers (nucleic bases) of native DNA; (iii) Compared to other electrode materials, the unique electronic structure of graphene sheets provides high electrical conductivity and highly localized electronic states at its edge,<sup>1</sup> enhancing the electron transfer rate between graphene and DNA.

#### **4. Conclusions**

To conclude, our study demonstrates for the first time, the immobilization, electro-oxidation and quantitative analysis of a monolayer of native DNA self-assembled on the vertically aligned graphene nanoflake films. The excellent electrocatalytic activity of graphene nanoflakes for the detection of dsDNA is believed to be strongly related with their dimension, nest-like surface structure, unique electronic structure and edge state. It can be envisioned that the use of GNFs as nanoconnectors, which establish direct electrical communication between the graphene edge plane and the active site of DNA or other biomolecules, will create a new generation of graphene-based enabling biotechnology leading to the production of label-free DNA biodetection, biofuel cells and electrocatalytic devices.

#### **Acknowledgements**

Authors acknowledge support from the Royal Society under the UK-China joint project (JP052544), the National Natural Science Foundation of China (21075003), the European Union under DESYGN-IT project (STREP Project 505626-1), EPSRC Portfolio Partnership Award,

EPSRC funded facility access to TEM in both the University of St Andrews and the University of Oxford (EP/F01919X/1).

## References

- [1] Y. Liu, X. Dong, P. Chen, *Chem. Soc. Rev.* 41 (2012) 2283.
- [2] N. Mohanty, V. Berry, *Nano Lett.* 8 (2008) 4469.
- [3] Y. Ohno, K. Maehashi, K. Matsumoto, *J. Am. Chem. Soc.* 131 (2010) 18012.
- [4] T.G. Drummond, M.G. Hill, J.K. Barton, *Nature Biotechnology* 21 (2003) 1192.
- [5] A. Erdem, P. Papakonstantinou, H. Murphy, *Analytical Chemistry* 78 (2006) 566.
- [6] E. Paleček, M. Bartošík, *Chem. Rev.* 112 (2012) 3427.
- [7] M. Fojta, *Electroanalysis* 14 (2002) 1449.
- [8] M. Muti, S. Sharma, A. Erdem, P. Papakonstantinou, *Electroanalysis* 23 (2011) 272.
- [9] O. Akhavan, E. Ghaderi, R. Rahighi, *ACS nano* 4 (2012) 2904.
- [10] M. Zhou, Y.M. Zhai, S.J. Dong, *Anal. Chem.* 81 (2009) 5603.
- [11] D.W. Pang, Y.P. Qi, Z.L. Wang, J.K. Cheng, J.W. Wang, *Electroanalysis* 7 (2005) 774.
- [12] S. Bollo, N.F. Ferreyra, G.A. Rivas, *Electroanalysis* 19 (2007) 833.
- [13] J.X. Wang, M.X. Li, Z.J. Shi, N.Q. Li, Z.N. Gu, *Electroanalysis* 16 (2004) 140.
- [14] K.B. Wu, J.J. Fei, W. Bai, S.S. Hu, *Anal. Bioanal. Chem.* 376 (2003) 205.
- [15] A. Özcan, Y. Sahin, M. Özsöz, S. Turan, *Electroanalysis* 19 (2007) 2208.
- [16] V. Brabec, *Biophys Chem.* 9 (1979) 289.
- [17] M.S. Goh, M. Pumera, *Analytical Chimica Acta* 711 (2012) 29.
- [18] A. Ambrosi, M. Pumera, *Phys. Chem. Chem. Phys.* 12 (2010) 8943.
- [19] M.S. Goh, A. Bonanni, A. Ambrosi, Z. Sofer, M. Pumera, *Analyst* 136 (2011) 4738.

- [20] M.L. Pedano, G.A. Rivas, *Biosensors and Bioelectronics* 18 (2003) 269.
- [21] A.M. Nowicka, E. Zabost, M. Donten, Z. Mazerska, Z. Stojek, *Bioelectrochemistry* 70 (2007) 440.
- [22] H.S. Wang, H.X. Ju, H.Y. Chen, *Electroanalysis* 13 (2001) 1105.
- [23] X. Cai, G. Rivas, P.A.M. Farias, H. Shiraishi, J. Wang, E. Plecek, *Electroanalysis* 8 (1996) 753.
- [24] N.G. Shang, P. Papakonstantinou, M. McMullan, M. Chu, A. Stamboulis, A. Potenza, S.S. Dhesi, H. Marchetto, *Advanced Functional Materials* 18 (2008) 3506.
- [25] S.R. Shin, C.K. Lee, I.S.J. Jeo, T.M. Kang, C. Kee, S.I. Kim, G.M. Spinks, G.G. Wallace, S.J. Kim, *Adv. Mater.* 20 (2008) 466.
- [26] A.A. Gorodetsky, J.K. Barton, *Langmuir* 22 (2006) 7917.
- [27] F. Boussicault, M. Robert, *Chem. Rev.* 108 (2008) 2622.
- [28] V. Brabec, Z. Balcarová, *Bioelectrochem. Bioenerg.* 9 (1982) 245.
- [29] V. Brabec, *Bioelectrochem. Bioenerg.* 7 (1980) 69.
- [30] B. Saoudi, C. Despas, M.M. Chehimi, N. Jammul, M. Delamar, J. Bessiere, A. Walcarius, *Sens. Actuators B* 62 (2000) 35.
- [31] R.L. McCreery, *Chem. Rev.* 108 (2008) 2646.

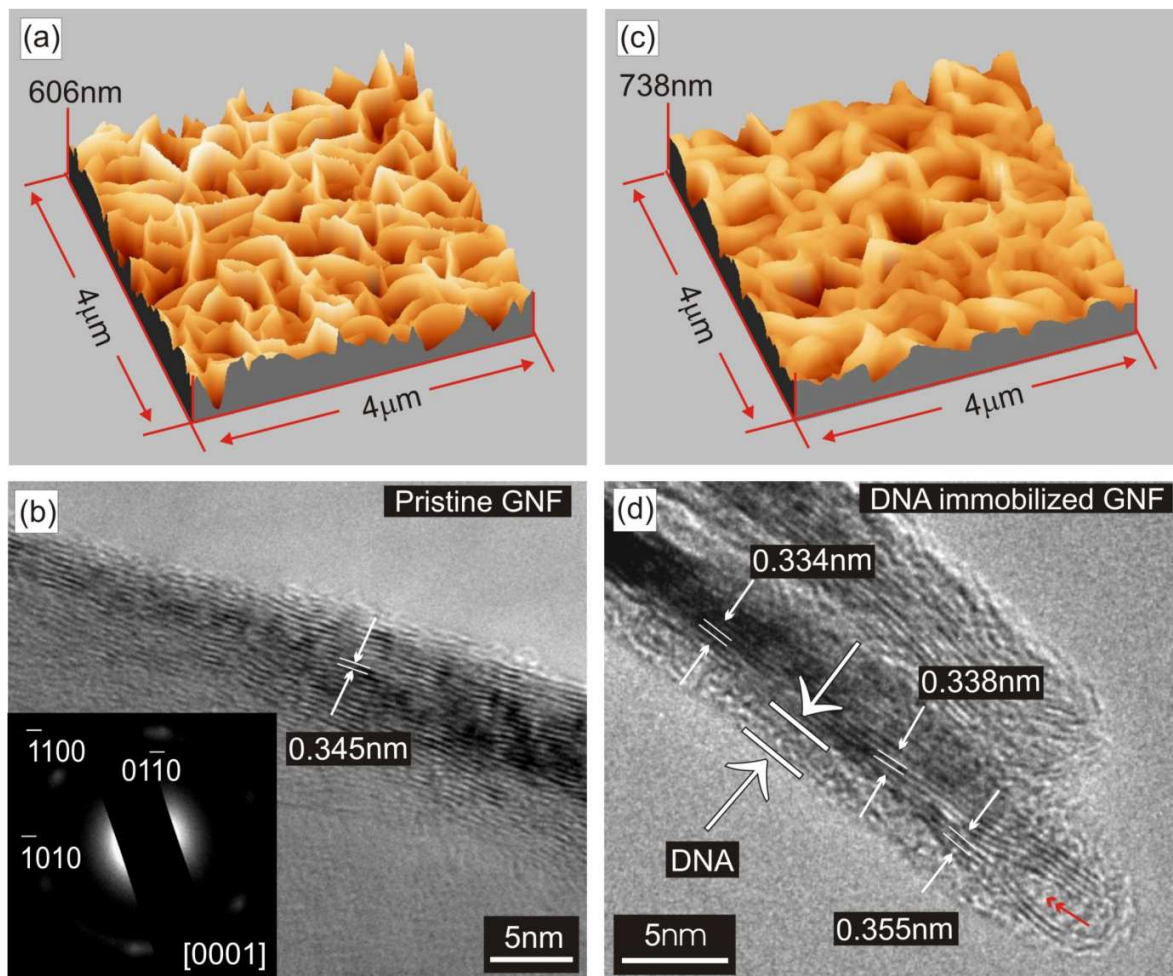


**Figure 1.** AFM (a) and TEM (b) images of pristine GNFs, the inset of (b) is the corresponding SAED pattern; AFM (c) and TEM (d) images of dsDNA immobilized GNFs.

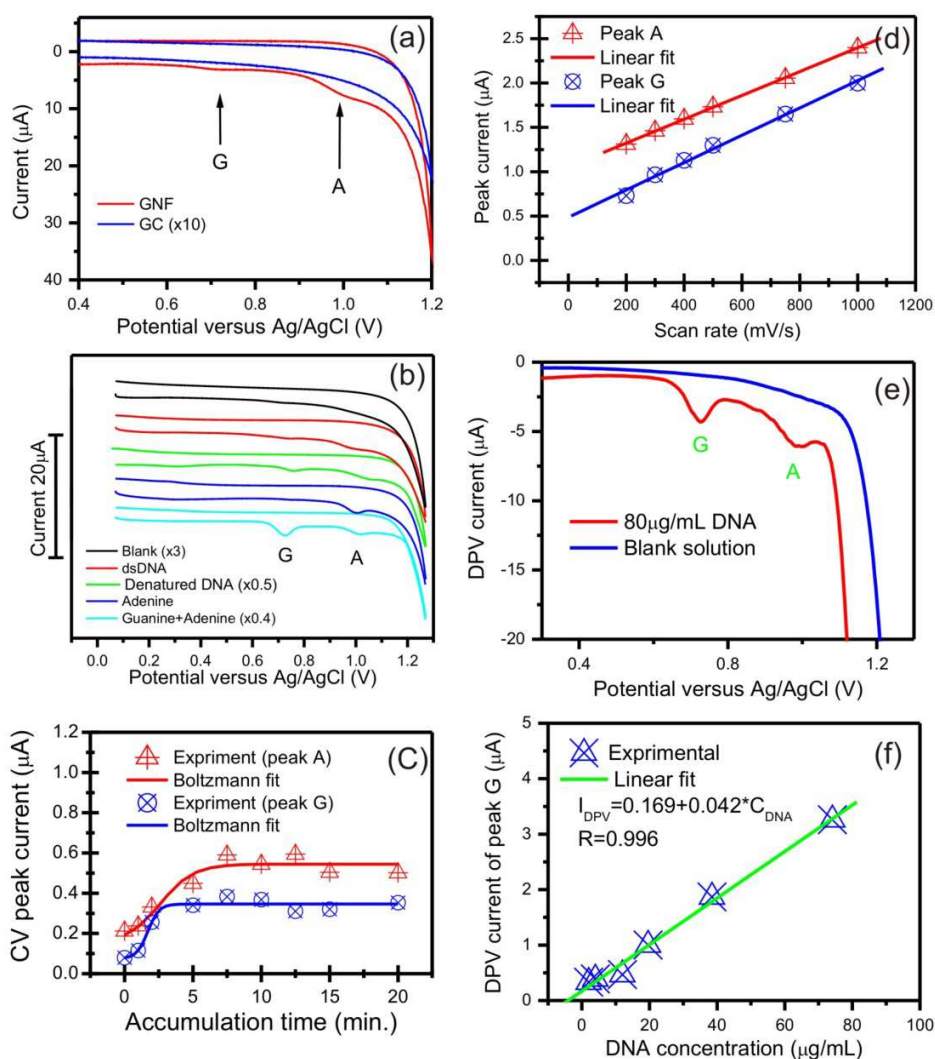


**Figure 2.** (a) CV profiles of the GC and GNF electrodes in the 0.5 mg mL<sup>-1</sup> fish sperm dsDNA solution at a scan rate of 0.1 Vs<sup>-1</sup>; (b) CV profiles of GNF electrodes in blank, 0.5 mg mL<sup>-1</sup> dsDNA, 0.5 mg mL<sup>-1</sup> denatured DNA, 0.5 μg mL<sup>-1</sup> adenine solutions and the mixture solution of 0.5 μg mL<sup>-1</sup> guanine and adenine at an accumulation time of 5 min. and a scan rate of 0.1Vs<sup>-1</sup>; (c) CV peak currents of dsDNA electrooxidation versus accumulation time; (d) CV peak currents of fish sperm dsDNA electrooxidation versus scan rate; (e) DPV profiles of GNF electrodes in blank and 80 μg mL<sup>-1</sup> fish sperm dsDNA solutions; (f) DPV currents of peak G as a function of fish sperm dsDNA concentration.